

# **TWO-DIMENSIONAL RECONSTRUCTION OF HEAT TRANSFER IN SURFACE COMBUSTION OF FLAT FLAME FURNACE GUIDED BY TDLAS TECHNOLOGY**

Shaofang Zhang<sup>1</sup>, Yuechun Wang<sup>1</sup>, Zengshan Bai<sup>1</sup>, Haroon Rashid<sup>2</sup>

<sup>1</sup>Shijiazhuang Vocational Technical College of Posts & Telecommunications, Shijiazhuang Hebei 050021, China

<sup>2</sup>Department of Structures & Environmental Engineering, University of Agriculture, Faisalabad, Pakistan

Email: [shaofangzh123@126.com](mailto:shaofangzh123@126.com)

---

**Abstract** – In order to study of application of tunable diode laser absorption spectroscopy (TDLAS) in the diagnosis of combustion heat transfer that is based on TDLAS and computed tomography (CT). A two-dimensional temperature distribution reconstruction system for surface combustion heat transfer field of flat flame furnace is established. Firstly, TDLAS technology and CT algorithm are studied. By selecting 7203.89 cm<sup>-1</sup> and 7435.62 cm<sup>-1</sup> absorption spectrum of water vapor, a two-dimensional reconstruction system of temperature measurement based on tunable diode laser absorption (2D) spectroscopy (TDLAT) is established. The system measurement results are verified. Secondly, the accuracy of the two-dimensional reconstruction image obtained by the system is analyzed. Finally, 2D reconstruction results are compared with the thermocouple test's results. The temperature measurement system established has been verified to be relatively stable with a small fluctuation range and a heating trend consistent with the set value. The analysis of reconstruction image accuracy shows that the reconstruction accuracy can be improved by increasing the number of laser paths and reducing the influence of noise. The reconstruction results of TDLAT have high accuracy, and the celebrity and timeliness of measurement have significant advantages in the online measurement of combustion diagnosis. The temperature measurement system of flat flame furnace based on TDLAT technology realizes the high-resolution and high-precision measurement of the combustion flame non-uniform flow field, which has important theoretical guidance, significance, and engineering experimental value for promoting the application of TDLAS technology in combustion flow field diagnosis.

**Keywords:** TDLAT Technology, Two-Dimensional Reconstruction, Flat Flame Furnace, Combustion Heat Transfer, Water Vapor.

---

## **1. Introduction**

Combustion is one of the most important ways to convert energy resources into energy. It will still exist widely in the current and future for quite a long time [1]. In the combustion process, temperature and gas component concentration are essential parameters to analyze the combustion state and chemical reaction process. Among them, temperature represents the amount of heat, the energy released in the combustion process the efficiency, and component concentration represents whether the fuel composition and combustion are completed [2]. To improve combustion efficiency and control pollution emissions, it is necessary to measure the proper distribution of temperature concentration and other flow field parameters in the combustion process [3].

The traditional flow field measurement technology mainly uses contact measurement method with a low cost. However, it has the disadvantages of slow measurement speed, low accuracy, inconvenient installation and carrying interference with the original flow field and so on [4]. At present, with the rapid development of related disciplines such as physics, chemistry, optics, electronics and semiconductor devices, the non-contact detection technology represented by apparitional analysis is used widely [5]. TDLAS technology uses low-cost semiconductor laser as the detection light source, with the advantages of a simple measurement system, easy miniaturization, strong anti-interference ability, etc. It has played an important role in the field of temperature, component concentration and speed measurement of combustion equipment such as high-temperature combustion furnace and engine [6].

Many scholars at home and abroad have done a lot of research on the diagnosis of combustion flow field based on TDLAS technology and achieved fruitful results. Zhang et al. (2018) studied using TDLAS technology to reconstruct the temperature and carbon dioxide concentration distribution in the axisymmetric methane downstream diffusion flame and also used the Abel inversion algorithm to reconstruct the two-dimensional (2D) distribution of attenuation coefficient, with higher inversion accuracy [7]. Buchholz et al. (2017) combined direct TDLAS technology with the first principle evaluation method to measure absolute water vapor. For the first time, the dual channel setting has realized a variety of self-verification functions [8]. In recent years, there are more and more researches on the combination of TDLAS and CT. In theory, the two reconstruction algorithms are improved accordingly. In the laboratory, the 2D distribution of uniform combustion field is measured with high resolution and high precision.

This study based on TDLAS technology, the average temperature inversion method under the desegregation of single optical path of flat flame furnace surface is studied. Then, combined with CT technology, the 2D plane visual monitoring of the surface temperature of the low flame furnace is apprehended by using the non-uniform distribution measurement system of the combustion flow field in the laboratory. As a result, this study lays the foundation for the measurement of the internal flow field of the engine combustion chamber and the combustion optimization of the coal-fired boiler.

## 2. Method

### 2.1 Basic principle of TDLAS technology

There are two methods of TDLAS temperature measurement: double line ratio method, Gauss broadening method and Boltzmann Atlas method. Among them, the Gaussian broadening method depends on the accurate measurement of the spectral broadening parameters, and the improvement of the accuracy is limited. The measurement of the nonuniform flow field distribution by Boltzmann Atlas method will increase the temperature slope, and the nonuniformity will be stronger. Which belongs to the category of direct absorption multi-line temperature measurement.

$$S(T) = S(T_m) \frac{Q(T_m) T_m}{Q(T) T} \exp\left[-\frac{hcE''}{k} \left(\frac{1}{T} - \frac{1}{T_m}\right)\right] \left[1 - \exp\left(-\frac{hcv_m}{kT}\right)\right] \left[1 - \exp\left(-\frac{hcv_m}{kT_m}\right)\right]^{-1} \quad (2)$$

In equation (2),  $Q$  is the total molecular partition function,  $h$  is the Planck constant,  $c$  is the speed of

Therefore, in this study, TDLAS double line temperature measurement method is selected. It has the advantages of high sensitivity and high accuracy to use the ratio of two absorption lines of the same target material to retrieve the temperature.

On a theoretical basis, TDLAS measurement is Beer-Lambert law. The absorption degree of matter is to different wavelengths of light, so it will cause the deviation of Beer-Lambert constant, so try to make the wavelength range of incident light narrow. When the frequency of the laser is the same as that of the absorption component of the measured gas, the energy of the laser will be absorbed. The schematic diagram of Beer-Lambert law is shown in Figure 1 [8]:

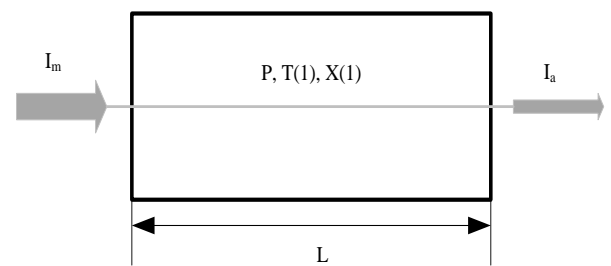


Figure 1: Beer-Lambert Law

As can be seen from Figure 1, when a laser beam with frequency  $\nu$  passes through the measured gas with length  $L$ , part of the light intensity is absorbed. The expression of the transmitted light intensity  $I_a$  after absorption is:

$$I_a = I_m \exp[-S(T)\Phi(\nu)PxL] \quad (1)$$

In equation (1),  $I_m$  is the light intensity without gas absorption, and  $I_a$  is the laser intensity after gas absorption in the measured area. In the equation,  $S(T)$  is the line strength of the absorption line,  $\text{cm}^2 \cdot \text{atm}^{-1}$ .  $\Phi(\nu)$  is the integral area normalized linear absorption function,  $\text{cm}$ .  $P$  is the measurement of ambient pressure,  $\text{atm}$ .  $x$  is the concentration of the substance (volume ratio of the target gas to the total gas).  $L$  is the absorption path,  $\text{cm}$ . The relationship between the line strength  $S(T)$  of the absorption line and the temperature  $T$  can be expressed as follows:

light,  $k$  is the Boltzmann constant, and  $E''$  is the low level of molecular transition.

From equation (2), it can be seen that the line strength is mainly affected by the partition function and the value of low state energy level, and in most cases, the product of the last two terms is almost unchanged, approximately 1. The corresponding integral absorbance A is:

$$A = \int_{-\infty}^{+\infty} -\ln\left(\frac{I_a}{I_m}\right)dv = S(T)PxL \tag{3}$$

$$R(T) = \frac{A_1}{A_2} = \frac{S_1(T)}{S_2(T)} = \frac{S_1(T_m)}{S_2(T_m)} \exp\left[-\frac{hc}{k}(E_1 - E_2)\left(\frac{1}{T} - \frac{1}{T_m}\right)\right] \tag{4}$$

It can be seen from equation (4) that the two-line temperature measurement is mainly through measuring the ratio of the integral absorbance of the two absorption lines to infer the temperature. There is greater the difference between the low-state energy levels of the two absorption lines, of the higher temperature measurement sensitivity.

### 2.2 Basic principle of CT technology

At present, many scholars combine TDLAS technology with CT to get 2D distribution image of combustion field according to the characteristics of non-uniformity of flow field. This method is called tunable diode laser absorption tomography (TDLAT).

The basic principles of CT technology are as follows. The X-ray source with a small bandwidth is taken and a photodetector is placed on the opposite side as the receiving device. The attenuated X-ray passing through the object is received by the detector. The intensity is  $I_m$ , and the incident intensity  $I_a$  of the X-ray source is measured. Then, in the same plane, the X-ray source and the photodetector are at the same time shifted by a certain number of steps N. After each translation, the incident intensity  $I_a$  and transmission intensity  $I_m$  are measured, and a group of data can be obtained after multiple translations. Then, in the same plane, the X-ray source and the detector are rotated by a small angle  $\Delta\varphi$  simultaneously, and the data of the angle is obtained by synchronously translating N steps. The above process is repeated. It is necessary to rotate  $N_\varphi$  times, make  $N_\varphi\Delta\varphi = 180^\circ$  rotation, and get  $N_\varphi$  group data. If the density of the object is unvarying, the linear attenuation coefficient of X-ray passing through the object is  $\mu$ . After the X-ray translation distance  $x$ , it decays to  $I_m$ . From the Beer-Lambert theorem, it can be obtained that:

$$I_m = I_a e^{-\mu x} \tag{5}$$

If the object is uniform, the linear attenuation coefficients of each segment are  $\mu_1, \mu_2, \mu_3$ , corresponding length is  $x_1, x_2, x_3$ . After substituting into equation (5), it can be obtained that:

When the gas medium is uniform, the temperature, concentration and optical path of the two absorption lines measured along the same optical path and the integral absorbance ratio is the ratio of the line strength. If there are two absorption lines, i.e. 1 and 2, the ratio of integral absorbance is:

$$\mu_1 x_1 + \mu_2 x_2 + \mu_3 x_3 \dots = \ln\left(\frac{I_a}{I_m}\right) \tag{6}$$

In fact, the interior plane of the object is not even. If the attenuation coefficient is  $\mu = \mu(x, y)$ , in a plane direction, the total attenuation along the path L is:

$$\int_L \mu dl = \ln\left(\frac{I_a}{I_m}\right) \tag{7}$$

This is called ray projection. If no specific translation path is specified, it shows that only one

direction along the plane, that is,  $\int_L \mu dl$  is called projection. It is a collection of sets of ray projections.

It can be seen from equation (7) that  $\int_L \mu dl$  can be obtained by measuring  $I_a$  and  $I_m$ . It is necessary to find the integrand  $\mu$  according to a series of

projections  $\int_L \mu dl$ . In this way, the image of  $\mu$  distribution can be obtained. This process is called reconstruction from projections, or X-CT imaging. The reconstructed image is a sectional image corresponding to the scanning plane.

### 2.3 Principle of spectral line selection

The key part of TDLAS technology is to select the spectrum line. The suitable spectrum line can improve the sensitivity and accuracy of detection, to improve the overall performance of the system. As the main product of hydrocarbon fuel combustion,  $H_2O$  is an ideal target gas. Moreover, in the near infrared band, there are a large number of strong absorption transition lines, which is very convenient for the use of commercial distributed feedback laser (DFB laser) in the communication band. The principle of selecting spectral lines is as follows:

1) Appropriate absorption lines are selected to make them have strong absorption in the range of measured temperature, and have a high signal-to-noise ratio;

2) The selected lines should be strong enough relative to the absorption lines around, and the absorption lines around should be as weak as possible;

3) The central wavelength of the spectral line is in the range of 1.25-1.65 $\mu$ m;

4) In the range of measured temperature, the ratio of spectral intensity should be a monotonic function of temperature;

5) The selected spectral pair has a high sensitivity in the temperature range to ensure the accuracy of measurement.

According to the above principles, two absorption lines of water vapor are selected according to the HITRAN spectrum database: 7203.89  $\text{cm}^{-1}$  and 7435.62  $\text{cm}^{-1}$ . The specific parameters of the spectrum are shown in Table 1.

Table 1: Spectral parameters of selected absorption lines

Line index	Transition frequency $\nu / \text{cm}^{-1}$	Wavelength $\lambda / \text{nm}$	Line strength $S / \text{cm}^{-1} \cdot \text{atm}^{-1}$	Lower state energy $E'' / \text{cm}^{-1}$
1	7203.89	1388.1	2.25e-21	724.08
2	7435.62	1344.9	5.83e-23	1557.85

The spectral parameters of HITRAN spectral database are used to perk up the absorbance of the two selected spectral lines at different temperatures,

$P = 1 \text{ atm}$ ,  $x = 0.05$ ,  $L = 10 \text{ cm}$ . The simulation curves are shown in Figures 2 and Figure 3.

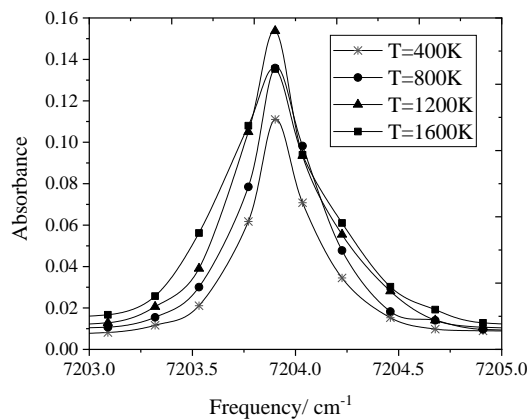


Figure 2: Absorbance simulation curve of 7203  $\text{cm}^{-1}$  ~ 7205  $\text{cm}^{-1}$

It can be seen from Figure 2 that there is no absorption interference near wave number 7203.89  $\text{cm}^{-1}$ , and there is a high absorption rate in high

temperature environment. Moreover, the higher the temperature, the stronger the absorption rate.

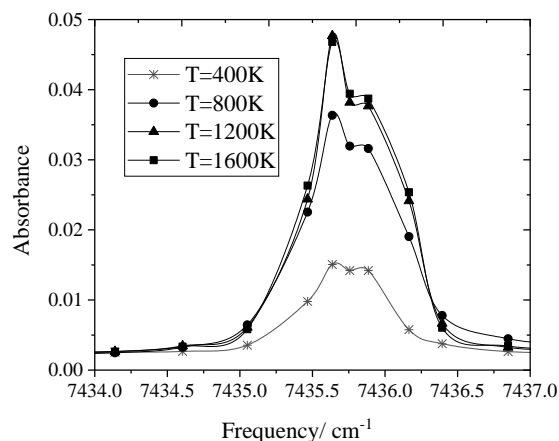


Figure 3. Absorbance simulation curve of 7434  $\text{cm}^{-1}$  ~ 7437  $\text{cm}^{-1}$

It can be seen from Figure 3 that the wave number is  $7435.62\text{ cm}^{-1}$ , and the absorption rate increases with the increase of temperature.

There is a small absorption peak near it.

Because of the small wave number interval, the absorption peak will not appear double peak phenomenon.

To sum up, it can be seen that the two absorption lines  $7203.89\text{ cm}^{-1}$  and  $7435.62\text{ cm}^{-1}$  have large line strength values, and the energy level difference of low transition state is large, and they have strong absorption capacity at high temperature, which meet the requirements of measuring signal-to-noise ratio (the average noise level of measurement system is about 1.5%), and do not overlap with the surrounding spectral lines [9-13].

## 2.4 Test device

In this research, TDLAS technology is combined with a computer tomographic CT algorithm to reconstruct the 2D combustion field on the surface of the flat flame furnace. Simultaneously, through simulation, the feasibility of the algorithm is verified, which lays the foundation for the subsequent measurement of the actual combustion field distribution. Taking methane / air premixed flat flame furnace as the temperature measurement object, it's fuel and oxygen are fully premixed before entering the combustion area, so it can produce one-dimensional characteristic stable standard flame. By controlling the equivalence ratio of the inlet air to control the combustion state, the combustion temperature in different states is simulated. The structure of the 2D reconstruction system of temperature measurement based on TDLAS technology is shown in Figure 4.

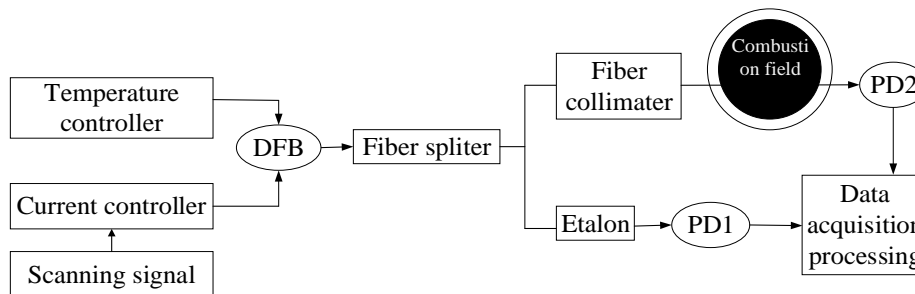


Figure 4. Two-dimensional reconstruction system of flat flame furnace temperature measurement based on TDLAS technology

As shown in Figure 4, DFB laser has been scanned with two absorption lines of  $7203.89\text{ cm}^{-1}$  (absorption line 1) and  $7435.62\text{ cm}^{-1}$  (absorption line 2). DFB laser is used in the experiment, and the output laser is divided into two channels by fiber beam splitter. One channel is directly received by detector PD1 through standard instrument (FSR = 315MHz) for wavelength calibration. The other way is transmitted to the combustion field to be tested by a single-mode fiber collimator, which is paralleled by the collimator, then transmitted through the area to be tested, and collected by the lens to PD2 for reception. After magnifying and adjusting the photocurrent signals of PDL and PD2, the upper computer controls the acquisition card for acquisition and post-processing.

After the 2D temperature distribution image is obtained from the above experiments, the reconstructed image quality is evaluated by normalized mean square distance D, normalized absolute distance R and normalized percentage

error%. Then, the reconstruction results are compared with the thermocouple test results. In the same temperature measurement section of flat flame furnace, thermocouple is used to measure flame temperature. B type thermocouple (BM100-100-110) shall be used. In the actual temperature measurement process of thermocouple, due to the influence of thermal radiation, experimental device and thermocouple arrangement on the combustion flow field, 121 thermocouples are arranged at most in the  $4\text{ cm} \times 4\text{ cm}$  measuring area, and the temperature is measured every 4mm.

## 3. Results and Discussion

### 3.1 Verification of high temperature furnace temperature measurement

In order to verify the feasibility of TDLAS temperature measurement system in this study, the experimental scheme is carried out on a high temperature tubular furnace.

A closed measuring area with comparatively constant temperature, concentration and pressure can be set for the high temperature tubular furnace for temperature measurement verification experiment. In the experiment, seven temperature steps are set: 800 ~ 1300K, one step every 100K. TDLAS technology is used to measure the temperature at different temperature steps. The results are shown in Figure 5:

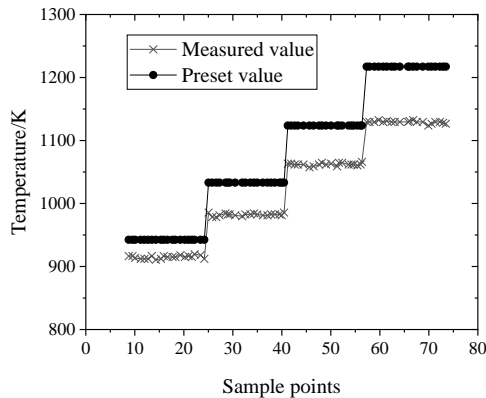


Figure 5. Comparison of temperature measurement results and setting results of high temperature tubular furnace

As can be seen from Figure 5, the measured value and the set value keep the same warming trend. Moreover, under the temperature gradient, the measured value is comparatively stable and the fluctuation range is smaller, within 10K.

Because the temperature measured by TDLAS is the average value along the whole path, the set temperature of the high-temperature furnace is the temperature value of its central area, and step by step reduced temperature section on both sides of the furnace tube pulls down the measured equivalent temperature value, so the measured temperature is lower than the actual set value, resulting in a system error. On the other hand, there is a geometric deviation between the thermocouple position of the furnace tube and the actual optical path, resulting in the measurement deviation.

### 3.2 Reconstruction accuracy analysis

The results of combustion field reconstruction are affected by many factors. Among them, the most important factors are the number of projection directions, the number of projection light and noise.

In the experiment, the number of each projection ray is fixed to 11, the number of projection slants are changed, and the reconstruction results under different projection slants are given, so as it is easy to analyze the influence of the number of projection directions on the reconstruction accuracy. If the number of projection slants decreases from 24 with tolerance of 5 to 4, the calculated criterion values of reconstruction results under different conditions are as shown in Table 2:

Table 2. Error of reconstruction caused by number of different projection directions

Projection angle	D(T)	D(C)	R(T)	R(C)	Error%(T)	Error%(C)
4	0.41	1.05	0.10	0.16	0.65	1.28
9	0.26	0.85	0.06	0.12	0.35	1.03
14	0.25	0.84	0.06	0.12	0.34	1.02
19	0.27	0.79	0.06	0.11	0.37	0.96
24	0.27	0.79	0.056	0.11	0.38	0.95

It can be seen from Table 2 that when the projection slant is above 9, the fluctuation of the three criteria is not very obvious, and the difference between their values is relatively small, which shows that when the number of projection slants reach a certain number (such as above 9 here), the

reconstruction quality is not sensitive to change the number of projection slants.

The number of projection angles is maintained at 19, and the number of parallel beams is set to increase from 11 to 27 with a tolerance of 4. The calculated criterion values of reconstruction results under different conditions are shown in Table 3:

Table 3: Error of different projection ray numbers to reconstruction

Parallel ray	D (T)	D(C)	R (T)	R (C)	Error% (T)	Error% (C)
11	0.26	0.85	0.06	0.12	0.34	1.03
15	0.19	0.78	0.04	0.09	0.25	0.82
19	0.18	0.72	0.04	0.09	0.23	0.80
23	0.18	0.69	0.04	0.08	0.23	0.79
27	0.17	0.66	0.04	0.08	0.22	0.77

It can be seen from Table 3 that with the increase of parallel beams, the change of that criterion is the trend of decreasing dispersion and single modulation, so the reconstruction quality is greatly affected by the analog beams in a single view. Therefore, in this process of practical application, the

more projection beams in the reconstruction area, give the higher reconstruction quality.

The number of experimental projection slants are set to 19. There are 11 analog beams at each angle. In the projection data, 5%, 10%, and 15% noise is added respectively, and the settlement criterion values under each noise level are shown in Table 4:

Table 4: Error of noise to reconstruction

Noise	D(T)	D(C)	R(T)	R(C)	Error%(T)	Error%(C)
0	0.28	0.87	0.06	0.13	0.39	1.06
5%	0.32	0.85	0.07	0.12	0.43	1.03
10%	0.46	0.86	0.10	0.13	0.59	1.02
15%	0.54	0.86	0.12	0.12	0.73	1.01

As can be seen from Table 4, with the increase of noise, the reconstruction error becomes larger and larger. For the combustion equipment such as flat flame furnace with stable combustion and large experimental space, the distribution reconstruction of filtered back projection field can be realized by arranging complete measuring beam around the furnace surface. In practical application, the circular symmetric flow field is a very common combustion flow field. Under this assumption, the projection data along different slants are axisymmetric. In the experiment, more than 9 projection slants can be selected. When the number of projection analog rays are as large as possible and the noise is as small as possible, the reconstruction measurement error can be reduced to the greatest extent, and the accurate reconstruction results of combustion temperature distribution can be obtained.

### 3.3 Verification of two-dimensional distribution measurement results

According to the assumed circular combustion field, 20 sets of projection data under single view are used to get 60 sets of projection data under single view. In the range of 0 degrees to 180 degrees, the projection at 180 slants of the range is considered.

Then, the algorithm proposed in this study is used to reconstruct the 2D temperature distribution image and compare it with the thermocouple

measurement results, as shown in Figure 6 and Figure 7:

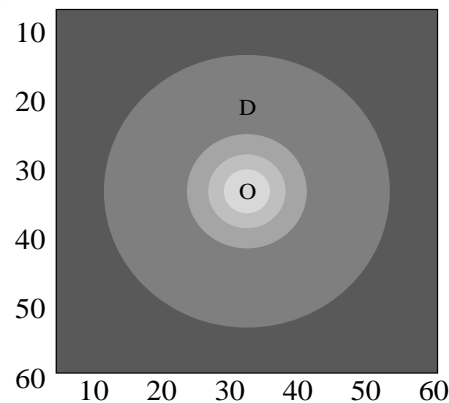


Figure 6: Two-dimensional temperature distribution of TDLAT measurement

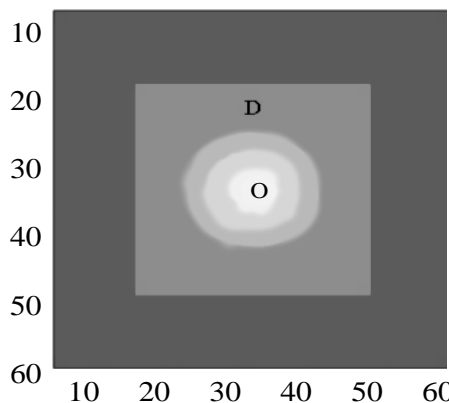


Figure 7: Temperature distribution of thermocouple measurement results

It can be seen from Figure 6 and Figure 7 that the temperature distribution between the two step by step changes in the same trend. The temperature at the center O is the highest, about 1700K, and the temperature at the edge D is lower, which is consistent with the flame combustion temperature of methane gas in laminar premixed environment. However, due to the difference in the number of reconstructed measuring points, the temperature of TDLAT reconstruction results can differ from 300 to 1700K, while the thermocouple measurement results cannot achieve this effect. This shows that TDLAT has the ability of fast reconstruction of high-resolution temperature field.

In order to verify the accuracy of TDLAT reconstruction temperature distribution,  $X = 0\text{mm}$  path in the measurement area is used. The TDLAT reconstruction results are compared with the thermocouple measurement results, as shown in Figure 8:

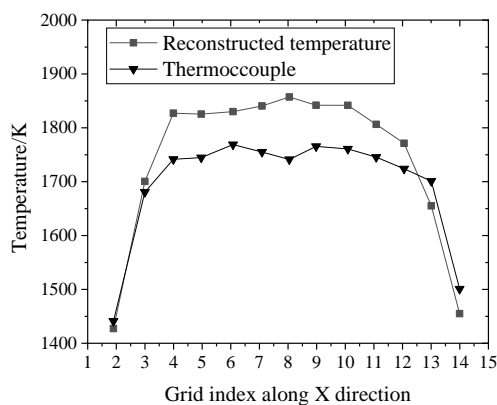


Figure 8: Comparison of thermocouple measurements and reconstruction results at several points along the X direction

It can be seen from Figure 8 that the temperature reconstruction result is generally higher than the thermocouple measurement value, but the deviation is not large, and the overall change trend is stable, which shows that the thermocouple measurement result is in good agreement with the TDLAS reconstruction result. It is mainly due to the influence of thermal radiation of thermocouple and the stability of flame that causes the error between the temperature measurement results of thermocouple and TDLAS. It can be seen from the above results that TDLAT has a high accuracy of temperature reconstruction. At the same time, the rapidity and timeliness of its measurement has a great advantage in the on-line measurement of combustion diagnosis.

## 4. Conclusions

In this study, the experimental equipment and 2D reconstruction results of the temperature measurement system of flat flame furnace surface combustion field based on CT technology and TDLAS technology are studied. The spectral database is used, and two absorption lines of  $\text{H}_2\text{O}$ :  $7203.89\text{ cm}^{-1}$  and  $7435.62\text{ cm}^{-1}$  are selected. At the same time, considering the correlation of temperature field, the 2D temperature distribution image can be reconstructed simultaneously. In the accuracy analysis, the effects of the number of projection directions, the number of projection rays and the noise on the reconstruction accuracy under different conditions are compared. The results show that the accuracy of CT reconstruction can be improved by increasing the number of laser paths and reducing the influence of noise. The 2D temperature distribution of flame in the measurement area of a flat flame furnace is obtained by using the modified  $\text{H}_2\text{O}$  spectrum database and CT algorithm. The results of TDLAT reconstruction are compared with those of thermocouple measurement, which shows that the results of TDLAT reconstruction have high accuracy. The advantages of this reconstruction method, such as rapidity, high precision and high resolution, are of great significance to the on-line measurement of combustion diagnosis. In the process of practical application, the distribution of temperature field along the axis is uneven, so TDLAS technology cannot accurately reflect the temperature distribution. In the later work, it is necessary to study the various combustion field of various gases.

## References

- [1] Qu Z, Holmgren P, Skoglund N, et al. Distribution of temperature,  $\text{H}_2\text{O}$  and atomic potassium during entrained flow biomass combustion-Coupling in situ TDLAS with modeling approaches and ash chemistry. *Combustion and Flame*, 2018, 188, pp. 488-497.
- [2] Sun P, Zhang Z, Li Z, et al. A study of two-dimensional tomography reconstruction of temperature and gas concentration in a combustion field using TDLAS. *Applied Sciences*, 2017, 7(10), pp. 990.
- [3] Liu C, Cao Z, Lin Y, et al. Online cross-sectional monitoring of a swirling flame using TDLAS tomography. *IEEE Transactions on Instrumentation and Measurement*, 2018, 67(6), pp. 1338-1348.
- [4] Dilip U Shenoy, Vinay Sharma, Shiva Prasad, H C. Strategic Evaluation In Optimizing The Internal Supply Chain Using Topsis: Evidence In A Coil-Winding Machine Manufacturer. *Acta*

- Mechanica Malaysia, 2020, 3(1): 1-4, DOI: 10.26480/amm.01.2020.01.04
- [5] S. Sathishkumar, M. Kannan Structural. Thermal and Thermo-Mechanical Analysis Of Four Stroke Petrol Engine Piston Using Cae Tools. Acta Mechanica Malaysia, 2020, 3(1): 5-10
- [6] Qasem Abu Al-Haija, Mohamad Musab Asad, Ibrahim Marouf, Ahmad Bakhuraibah, Hesham Enshasy. FPGA Synthesis and Validation of Parallel Prefix Adders. Acta Electronica Malaysia, 2019, 3(2): 31-36.
- [7] Sheeza Ishtiaq, Ahthasham Sajid, Raja Asif Wagan. Review Paper on Wearable Computing its Applications and Research Challenges. Acta Electronica Malaysia, 2019, 3(2): 37-40.
- [8] Ihtisham ul Haq. Analytical Approximate Solution Of Non-Linear Problem By Homotopy Perturbation Method (Hpm). Matrix Science Mathematic, 2019, 3(1): 20-24.
- [9] Bürkle S, Biondo L, Ding C P, et al. In-cylinder temperature measurements in a motored IC engine using TDLAS. Flow, Turbulence and Combustion, 2018, 101(1), pp. 139-159.
- [10] Jeon M G, Deguchi Y, Kamimoto T, et al. Performances of new reconstruction algorithms for TDLAT (computer tomography-tunable diode laser absorption spectroscopy). Applied Thermal Engineering, 2017, 115, pp. 1148-1160.
- [11] Ghorbani R, Schmidt F M. ICL-based TDLAS sensor for real-time breath gas analysis of carbon monoxide isotopes. Optics express, 2017, 25(11), pp. 12743-12752.
- [12] Zhang G, Wang G, Huang Y, et al. Reconstruction and simulation of temperature and CO<sub>2</sub> concentration in an axisymmetric flame based on TDLAS. Optik, 2018, 170, pp. 166-177.
- [13] Mayerhöfer T G, Mutschke H, Popp J. Employing Theories Far beyond Their Limits—The Case of the (Boguer-) Beer–Lambert Law. ChemPhysChem, 2016, 17(13), pp. 1948-1955.